



Open Archive Toulouse Archive Ouverte

OATAO is an open access repository that collects the work of Toulouse researchers and makes it freely available over the web where possible

This is an author's version published in: <http://oatao.univ-toulouse.fr/20663>

Official URL:

<https://doi.org/10.1080/10407789608913860>

To cite this version:

Khallouf, Hicham and Gershuni, Grigori Z. and Mojtabi, Abdelkader Some properties of convective oscillations in porous medium. (1996) Numerical Heat Transfer, Part A: Applications, 30 (6). 605-618. ISSN 1040-7782

Any correspondence concerning this service should be sent to the repository administrator: tech-oatao@listes-diff.inp-toulouse.fr

SOME PROPERTIES OF CONVECTIVE OSCILLATIONS IN POROUS MEDIUM

H. Khallouf

UMR CNRS/INP-UPS 5502, Université Paul Sabatier, 118 Route de Narbonne,
31062 Toulouse Cedex, France

G. Z. Gershuni

Department of Theoretical Physics, Perm State University, Bukirev Str. 15,
614600 Perm, Russia

A. Mojtabi

UMR CNRS/INP-UPS 5502, Université Paul Sabatier, 118 Route de Narbonne,
31062 Toulouse Cedex, France

Convective oscillations in porous media are studied numerically. A two-dimensional square, differentially heated cavity, filled with a saturated porous medium, is considered subject to linear harmonic oscillations in the vertical direction. The formulation is based on the Darcy-Boussinesq model. The problem includes three nondimensional parameters: the Rayleigh number for porous media Ra , its vibrational analog Ra_v , and the nondimensional frequency f . The time-dependent Darcy-Boussinesq equations have been solved using a pseudo-spectral Chebyshev collocation method. The instantaneous fields of the established oscillatory regimes are presented. Also, some instantaneous and mean characteristics are studied and discussed. The distinctions from the case of viscous fluid alone are emphasized.

INTRODUCTION

This article is devoted to the study of streaming phenomenon in a fluid-saturated porous enclosure induced by oscillatory body forces. Our statement of the problem is close to that of Refs. [1] and [2] but is formulated for the case of a porous medium rather than for viscous fluid. This means that, unlike the case of viscous fluid, one cannot expect the resonance phenomenon, which takes place in the range of the nondimensional angular frequency $\omega \in [10^2, 10^3]$. In fact, when the cavity, filled with viscous fluid, vibrates harmonically in the presence of temperature inhomogeneity, regular mean flows appear (the effect of vibrational convection [3, 4]). In the case of a porous medium, the effect of vibrational convection, as is demonstrated here, also exists but only in the case of finite

This work was supported, in part, by CNES (Centre National d'Etudes Spatiales).

Address correspondence to Professor A. Mojtabi, Laboratoire de Modelisation en Mecanique de Fluides, Institut de Mecanique des Fluides, Université Paul Sabatier, 118 Route de Narbonne, 31062 Toulouse Cedex, France.

NOMENCLATURE

a	cavity side	x, y	coordinates
b	displacement amplitude	β	coefficient of thermal expansion
f	frequency	Θ	temperature at $x = 0$
Nu	Nusselt number ($= - \int_0^1 \partial T / \partial x _{x=0} dy$)	ν	kinematic viscosity
\mathbf{k}	unit vector of the axis of vibrations	ρ	density
K	coefficient of permeability	χ	effective heat diffusivity
p	pressure	ψ	stream function
r	ratio between heat capacities	ω	angular frequency of vibration
Ra	thermal Rayleigh number ($= g \beta \Theta Ka / \nu \chi$)	Subscript	
Ra_v	vibrational Rayleigh number ($= b \hat{\omega}^2 \beta \Theta Ka / \nu \chi$)	max	maximum value
t	time	Superscript	
T	temperature		
\mathbf{u}	velocity vector	n	time level

frequencies. In the limiting case of high frequency, we find that this effect disappears as a result of the simplifications adopted in the Darcy model. Generally speaking, the porous medium is an example of dynamical systems with a high level of dissipation. This leads to smoothing of all oscillatory phenomena.

As an exception, we can say that the oscillatory motions that appear in porous media are the result of equilibrium convective instability in the presence of some specific complications, such as in the case when the fluid saturating the medium is a binary mixture [5, 6], or when convection appears in the basic state with the transversal-horizontal flow [7, 8]. In addition, a well-studied problem is that of oscillatory convection that occurs under the action of a static gravity field at high Rayleigh numbers. This latter problem has been the subject of several investigations in the case of finite boxes heated from below [9, 10].

In this work we consider the convective oscillations of the fluid in porous media due to vertical vibrations of a square cavity in the presence of a lateral temperature gradient. The instantaneous fields of filtration velocity and temperature are presented. Some integral characteristics such as mean temperature, heat flux, mean stream function, and kinetic energy of the mean flow are studied as a function of representative values of the nondimensional parameters. Thus we are interested in some special case of g-jitter theory for porous media.

PROBLEM DESCRIPTION

Consider a fluid-saturated porous medium enclosed in a two-dimensional square cavity of side a (see Figure 1). The vertical walls at $x = 0$ and $x = a$ are kept at constant temperatures Θ and 0, respectively, where the horizontal walls are thermally insulated. All the boundaries are assumed to be rigid and impermeable. The entire system, including the cavity and the porous medium, oscillates along the vertical axis following the displacement law $[b \sin(\hat{\omega} t)\mathbf{k}]$, where b is the displacement amplitude, $\hat{\omega}$ is its angular frequency, and \mathbf{k} is the unit vector directed

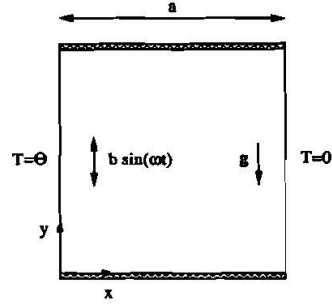


Figure 1. Physical configuration.

upward. The convective filtration can be described within the Darcy-Boussinesq model written in the proper (oscillating) coordinate system. Thus the gravity field has to be replaced by the sum of the gravity and the vibrational acceleration,

$$\mathbf{g} \rightarrow \mathbf{g} + b\hat{\omega}^2 \sin(\hat{\omega}t)\mathbf{k} \quad (1)$$

in the momentum equation.

Using the velocity of filtration $\mathbf{u} = (u_x, u_y)$, the pressure p , and the temperature T as independent variables, the equations of the Darcy-Boussinesq model are

$$\frac{\nu}{K}\mathbf{u} + \frac{1}{\rho}\nabla p = \beta T(\mathbf{g} + b\hat{\omega}^2 \sin \hat{\omega}t)\mathbf{k} \quad (2)$$

$$\nabla \cdot \mathbf{u} = 0 \quad (3)$$

$$r\frac{\partial T}{\partial t} + \mathbf{u} \cdot \nabla T = \chi \nabla^2 T \quad (4)$$

here ν is the kinematic viscosity of the fluid, χ is the effective heat diffusivity, β is the coefficient of thermal expansion, ρ is the reference value of density (constant), \mathbf{k} is the unit vector directed vertically upward, K is the coefficient of permeability, and r is the ratio of the heat capacity of the medium to that of the fluid.

The boundary conditions are

$$\begin{aligned} x=0 \quad (0 \leq y \leq a) \quad u_x &= 0 \quad T = \Theta \\ x=a \quad (0 \leq y \leq a) \quad u_x &= 0 \quad T = 0 \\ y=0, a \quad (0 \leq x \leq a) \quad u_y &= 0 \quad \frac{\partial T}{\partial y} = 0 \end{aligned} \quad (5)$$

The nondimensional form of the equation system and the boundary conditions is introduced using the following characteristic quantities: a for length, χ/a for

velocity of filtration, ra^2/χ for time, and Θ for temperature. In order to simplify the presentation the same notation has been used for the nondimensional variables. Thus we obtain the following nondimensionalized form of the system of equations:

$$\mathbf{u} + \nabla p = T(Ra + Ra_v \sin \omega t)\mathbf{k} \quad (6)$$

$$\nabla \cdot \mathbf{u} = 0 \quad (7)$$

$$\frac{\partial T}{\partial t} + \mathbf{u} \cdot \nabla T = \nabla^2 T \quad (8)$$

The boundary conditions are

$$\begin{aligned} x = 0 \quad (0 \leq y \leq 1) \quad u_x = 0 \quad T = 1 \\ x = 1 \quad (0 \leq y \leq 1) \quad u_x = 0 \quad T = 0 \\ y = 0, 1 \quad (0 \leq x \leq 1) \quad u_y = 0 \quad \frac{\partial T}{\partial y} = 0 \end{aligned} \quad (9)$$

The problem includes three nondimensional parameters: the filtration Rayleigh number corresponding to natural convection in porous media Ra , the vibrational analog Ra_v , and the nondimensional frequency ω , such that

$$Ra = \frac{g\beta\Theta Ka}{\nu\chi} \quad Ra_v = \frac{b\hat{\omega}^2\beta\Theta Ka}{\nu\chi} \quad \omega = \frac{ra^2}{\chi} \hat{\omega} \quad (10)$$

For convenience of presentation, the nondimensional frequency $f = \omega/2\pi$ is always used instead of ω , the angular pulsation.

The initial value problem, Eqs. (6)–(8), determines the solution of the initial problem with the boundary conditions, Eq. (9). Hereafter our attention is focused on the time-periodic established regimes that take place after a transit process for moderate values of the parameters. In addition to the instantaneous fields of temperatures and stream function ψ , we are interested in mean characteristics of the flow in a time-averaging sense. Here, for a given function h , an overbar is used to denote average value over the period (τ) of forcing:

$$\bar{h}(x, y) = \frac{1}{\tau} \int_0^\tau h(x, y, t) dt$$

The origin of the time integration coincides with the beginning of a vibration cycle in the asymptotic regime.

An important characteristic is heat flux through the cavity given by the Nusselt number Nu . Its instantaneous value is

$$Nu(t) = - \int_0^1 \frac{\partial T}{\partial x} \Big|_{x=0} dy$$

Another important characteristic for the description of thermovibrational convection is

$$E = \frac{1}{2} \int_0^1 \int_0^1 \bar{\mathbf{u}}^2 dx dy$$

which is the kinematic energy of the mean flow.

NUMERICAL METHOD

In this section we give a brief description of the numerical method employed herein, and proof of its accuracy when applied to a problem of natural convection in a differentially heated square cavity (our physical configuration) filled with a porous medium. The time-dependent equations, Eqs. (6)–(8), are discretized in time using a second-order finite difference scheme. Equations (6) and (3) are simply written at time $t^{n+1} = (n+1)\Delta t$, where n is the time level and Δt is the time step. The advection-diffusion energy equation is approximated semi-implicitly using an implicit second-order Euler backward scheme for linear terms and an Adams-Bashforth method for the nonlinear term. Hence, in the order of their solutions, the semidiscrete equations read as follows:

$$\nabla^2 T^{n+1} - \frac{3}{2\Delta t} T^{n+1} = - \frac{2T^n - \frac{1}{2}T^{n-1}}{\Delta t} + [2(\mathbf{u} \nabla T)^n - (\mathbf{u} \nabla T)^{n-1}] \quad (11)$$

$$\mathbf{u}^{n+1} + \nabla p^{n+1} = (Ra + Ra_v \sin \omega t_{n+1}) T^{n+1} \mathbf{k} \quad (12)$$

$$\nabla \cdot \mathbf{u}^{n+1} = 0 \quad (13)$$

A high-accuracy spectral method, namely, the Chebyshev collocation method [11], with the Gauss-Lobatto zeros as collocation points, is used to solve the Helmholtz problem, Eq. (11), and the projection problem, Eqs. (12) and (13). To discretize the projection problem, we utilize the Darcy solver developed in Ref. [12] (also see Ref. [13] for a full description of the spatial discretization). The well-known successive diagonalizations technique is implemented to invert the corresponding operators. We must mention here that the Darcy-Euler solver is direct and guarantees a spectral accuracy solution with free divergence for the \mathbf{u} field on the whole domain, including the boundaries.

In this study, we limit ourselves to relatively small values of Ra and Ra_v ($Ra \leq 200$, $Ra_v \leq 500$). The accuracy of the numerical method is studied for a static natural convection problem. In Table 1 are given ψ_{\max} and Nu for increasing mesh refinement (polynomial degree) at $Ra = 500$ and 1000 . It can be noted that Nu is more sensitive than ψ to the numerical resolution.

Table 1. Effects of polynomial degree on Nu and the maximum value of ψ

N	Nu		ψ_{max}	
	Ra = 500	Ra = 1000	Ra = 500	Ra = 1000
20	9.1101	14.652	13.540	20.470
26	8.9916	13.875	13.539	20.489
30	8.9788	13.729	13.540	20.489
36	8.9796	13.652	13.540	20.489

A high spectral convergence, up to the fourth digit for the two presented values of Ra, is obtained when N exceeds 30° in each direction. All the numerical results presented in the next section have been carried out using 30^2 polynomial modes.

RESULTS AND DISCUSSION

Before the results of our numerical simulations are presented, it is worthwhile to recall some known symmetry properties of the flow structures that are expected to be retained for both instantaneous and time-averaged fields. The static natural convection flows possess the centrosymmetry property generated by the operator $S_x S_y$, where S_x and S_y stand for the reflection symmetries:

$$S_x[\psi(x, y), T(x, y)] = [-\psi(1 - x, y), 1 - T(1 - x, y)]$$

$$S_y[\psi(x, y), T(x, y)] = [-\psi(x, 1 - y), T(x, 1 - y)]$$

Further, we divide our results into two parts. Our goal in the first part is to analyze the response of the system in the absence of a static field in order to illustrate thermovibrational convection in porous media. The second part is concerned with the interaction between static natural convection and the thermovibrational mechanism.

Flow Regimes Under the Condition of Weightlessness

We begin our explanation of the results from the case of the weightlessness state (i.e., $Ra = 0$). A detailed description is given at $Ra_v = 200$; nevertheless, it has been verified that this description holds qualitatively for a large range of Ra_v (up to $Ra_v = 1000$). Concerning the flow structures, a general picture applies independently of both the frequency and the vibrational Rayleigh number. At every moment the solution possesses the centrosymmetry property $S_x S_y$ as steady natural convection flow. In addition, oscillations of all the variables have time symmetry with respect to the middle of the cycle. In particular,

$$\psi\left(x, y, t + \frac{\pi}{\omega}\right) = S_x[\psi(x, y, t)] = S_y[\psi(x, y, t)]$$

$$T\left(x, y, t + \frac{\pi}{\omega}\right) = S_y[T(x, y, t)]$$

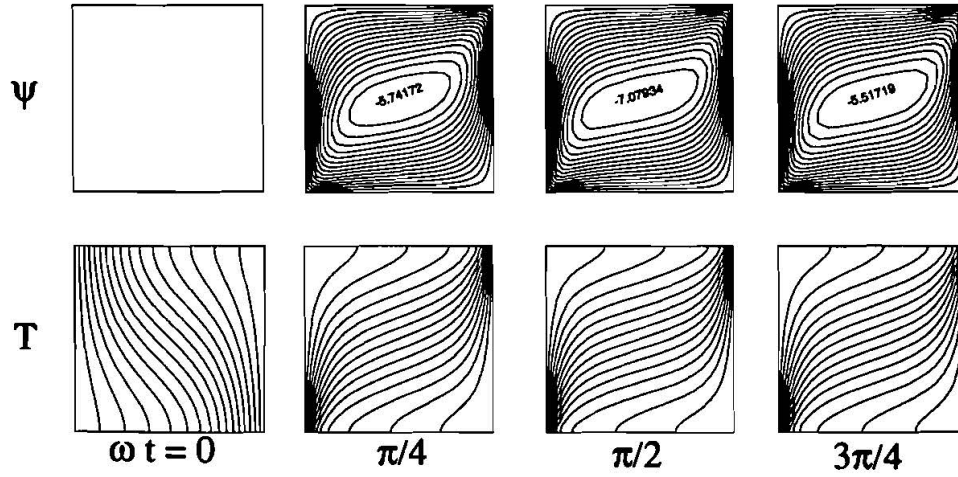


Figure 2. Time sequence of ψ and T at $Ra = 0$, $Ra_v = 200$ with $f = 1$, over the first half of a vibration cycle at intervals of $\omega t = \pi/4$.

The latter equation implies that for a forcing of period τ the Nusselt number is $\tau/2$ periodic. Furthermore, it is straightforward to show that the mean fields of temperature and stream function possess the reflection symmetries S_x and S_y .

In Figures 2 and 3, diagrams of the stream function and the isotherms are presented during the first half of an oscillating cycle ($\omega t \in [0, \pi]$) at frequencies of 1 and 400, respectively. The aforementioned symmetries allow for extension to the whole cycle. Two different dynamical behaviors can be recognized, correspond-

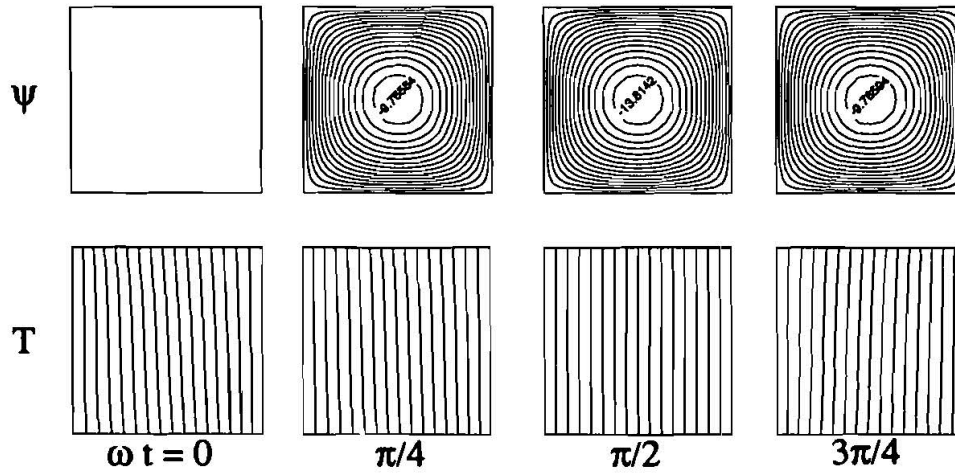


Figure 3. Time sequence of ψ and T at $Ra = 0$, $Ra_v = 200$ with $f = 400$, over the first half of a vibration cycle at intervals of $\omega t = \pi/4$.

ing to the two limiting cases ($f \rightarrow 0$) and ($f \rightarrow \infty$) usually considered when studying the thermovibrational convection of fluids (see, for instance, Refs. [14] and [15]). Obviously, at very low frequencies, the rate of time evolution of temperature can be neglected; thus the diffusion mechanism dominates heat transport. From a dynamical point of view the time-dependent convection at a given time t_0 corresponds to the steady convection due to a static source of amplitude $Ra_v \sin \omega t_0 T k$. This constitutes the so-called quasi-static regimes [14, 15]. Furthermore, ψ and T oscillate in phase with the forcing, as is shown in Figure 2 for $f = 1$, although for a slight phase difference between T and the source (see the diagrams at $t = 0$).

The opposite limiting case ($f \rightarrow \infty$) is represented in Figure 3 for $f = 400$. The most important result is the damping of the temperature oscillation, which is reduced to a small sinusoidal perturbation around the conductive solution. Also, this perturbation is in phase quadrature with the source, since at $\omega t = \pi/2$ the solution is perfectly conductive. A description of the time-dependent response when the frequency varies from low to high values is given in Figure 4 where the periodic oscillations of the stream function in the center of the cavity and the Nusselt number are presented versus the phase ωt . A quasi-synchronous response is obtained at $f = 1$. The increase of the phase difference between Nu and the source is accompanied by damping of the magnitude of Nu when the frequency increases. The amplitude of ψ is subject to small variation up to $f = 20$. When this value is exceeded, ψ becomes independent of f , and the curves corresponding to $f = 20, 100$, and 200 collapse into one sinusoidal curve.

The mean values of the stream function $\bar{\psi}$ and isothermals \bar{T} are depicted in Figure 5 for increasing frequencies ($f = 10, 20, 100$, and 400). This demonstrates the effect of vibrational convection in porous media, where a regular mean flow is obtained at relatively low frequencies. The quadrupole flow structure illustrates the reflection symmetries S_x and S_y , as mentioned above. We see that the flow intensity decreases monotonously as far as f increases. Accordingly, the temperature fields tend to a conductive regime. The effect of vibrational convection disappears when $f \rightarrow \infty$.

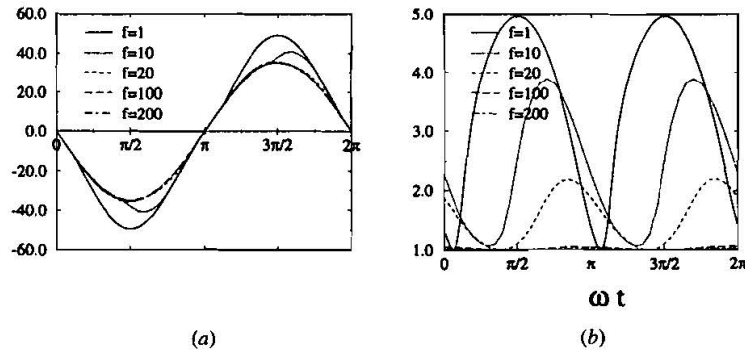


Figure 4. Periodic oscillations of (a) ψ in the center of the cavity and (b) Nu at $Ra_v = 200$, $Ra = 0$, and various frequencies.

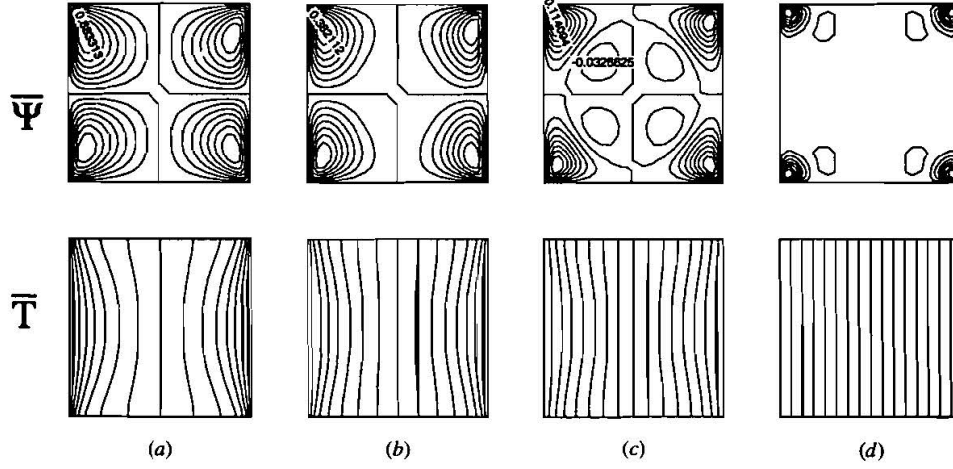


Figure 5. Structures of the mean fields of stream function and temperature at $Ra_v = 200$, $Ra = 0$, and frequencies (a) 10, (b) 20, (c) 100, and (d) 400.

Figures 6a and 6b summarize the results for the case of weightlessness. The evolutions of the kinetic energy of the mean flow E and the averaged Nusselt number \bar{Nu} given as functions of the frequency f for various values of Ra_v . Each of these characteristics decreases with frequency, and in the limiting case $f \rightarrow \infty$, an asymptotic behavior can be derived. In fact, the asymptotics $E \sim f^{-4}$ and $(\bar{Nu} - 1) \sim f^{-2}$ are valid whatever the value of Ra_v .

The results established here are similar to those obtained in the case of a fluid-filled cavity, but at low frequencies and small amplitude of vibration (see Refs. [1] and [14]). In the case of viscous fluid, when the amplitude of vibrations is high enough, the inertial effects allow the temporal symmetry to break around the middle of the period, leading to a frequency resonance. The present results show that there is no significant resonance phenomenon in porous media.

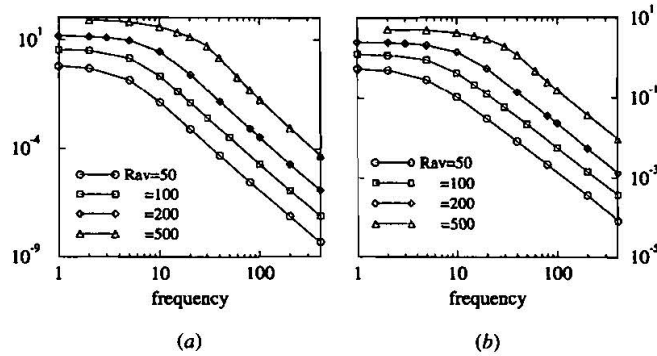


Figure 6. Kinetic energy of the (a) mean flow and (b) mean Nusselt number versus the frequency ($Ra = 0$, $Ra_v = 200$).

Modulated Gravity Flow Regimes

Let us consider now the case of a modulated gravity field ($Ra \neq 0$). Our aim is to analyze the interaction between natural and vibrational convection. In all the numerical results presented hereafter, the Rayleigh number was fixed ($Ra = 200$), the parameters of our investigations are Ra_v ($Ra_v \in \{100, 200, 300, 400, 500\}$), and the nondimensional frequency ($f \in [1, 400]$). Notice that since $Ra \neq 0$, the symmetry of the forcing with respect to the middle of the cycle is lost. Consequently, the spatial flow structure retains only the centrosymmetry ($S_x S_y$) for both instantaneous and mean fields.

First, we present a general description of the mean characteristics E and \overline{Nu} as functions of f . These variables are depicted in Figures 7a and 7b, respectively. It is seen that at low values of Ra_v ($Ra_v/Ra \leq 1$), the static natural convection flow is insignificantly influenced by the vibrations over the entire range of frequencies considered here. The deviation of the mean heat flux is less than 15% from its value of the static case. An important effect of vibrations is observed when $Ra_v/Ra \geq 2$. For these values of Ra_v the numerical results suggest that the most important modifications of heat flux and flow intensity occur in the region of low frequencies (Figure 7). This matches well the results carried out under the condition of weightlessness, where the maximum thermovibrational convection is obtained at low frequencies. The evolution of \overline{Nu} is nonmonotonous, where at $Ra_v = 500$ and $f = 1$ the mean heat flux is increased more than 30% from its value in the static case. Then it decreases to attain a minimum value lower than the static heat flux. Further, the same figure shows that convergence toward static values is achieved when f is increased independently of Ra_v .

This behavior is reflected in the structures of the mean flow (stream function and isotherms), where we found that for $Ra_v/Ra \leq 1$ the basic state flow dominates the convective filtration. Hence, we describe only the spatial structure for higher values of Ra_v when the thermovibrational effect is high enough. In Figure 8 are given the diagrams of $iso-\bar{\psi}$ and $iso-\bar{T}$ at $Ra = 200$ and $Ra_v = 500$ and four

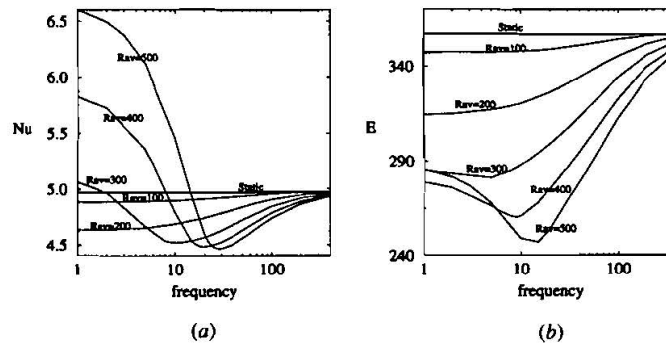


Figure 7. Kinetic energy of the (a) mean flow and (b) mean Nusselt number at $Ra = 200$ and various values of Ra_v versus the frequency.

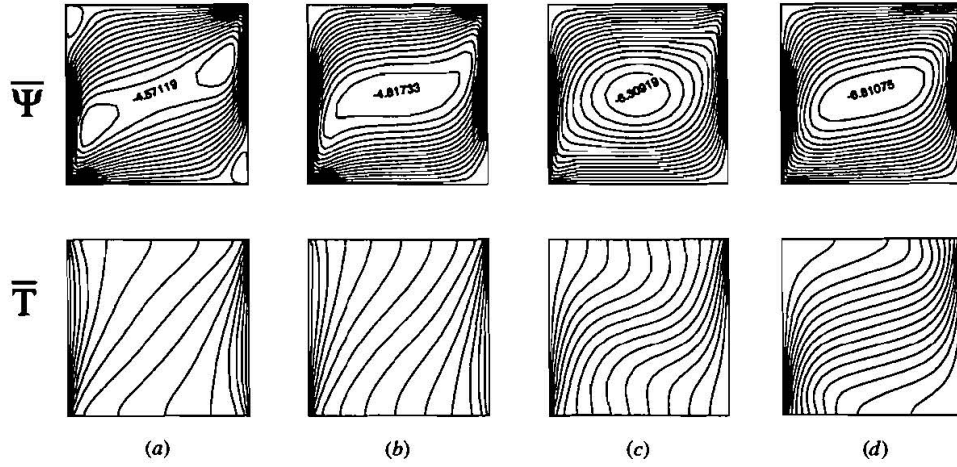


Figure 8. Structures of the mean stream function and the isotherms at $Ra = 200$ and $Ra_v = 500$, with a frequency of (a) 1, (b) 10, (c) 25, and (d) 100.

values of the frequency ($f = 1, 10, 25, 100$). The intensive interaction between the natural (one-cell) and vibrational (four-cells) convection mechanism leads to important modifications in the spatial structure at low frequencies. Roughly speaking, the two clockwise rotating cells of the quadrupole (see Figure 5) induce acceleration of the flow in the lower left and upper right corners; the others (counterclockwise) are reduced to two small recirculations in the corresponding corners (Figure 8a). The overall interaction results in a decrease of the main cell intensity.

Increasing the frequency (Figures 8a–8c) causes suppression of the two counterclockwise recirculations, whereas the intensity of the clockwise (natural) cell increases gradually to reach its value of the static regime. Also, at $f = 100$ (Figure 8d) one can distinguish the well-known natural convection structure. The evolution of the isotherms presented in the same figure (right) is in conformity with that of $\bar{\psi}$. The dominance of the thermovibrational mechanism in heat transport is clearly identified at $f = 1$, where the structure of the isotherms looks like that at $Ra = 0$ with a distortion (clockwise rotation) due to the principal circulation. At this frequency the usual horizontal stratification in natural convection is destroyed. As the frequency increases, the horizontal stratification in the core region is reestablished.

The instantaneous fields at $f = 10$ and $f = 400$ are presented in Figures 9 and 10, respectively. The description of these results is the same as in the case of weightlessness except that the oscillation takes place around the static structure. Thus at $f = 10$, high-magnitude vibrations of ψ and T are noticed. An inversion of the rotation direction occurs when $\omega t \in [\pi, 5\pi/4]$. At $f = 400$ the rotation direction changes; even so, the isotherms are nearly the same as those obtained with static convection.

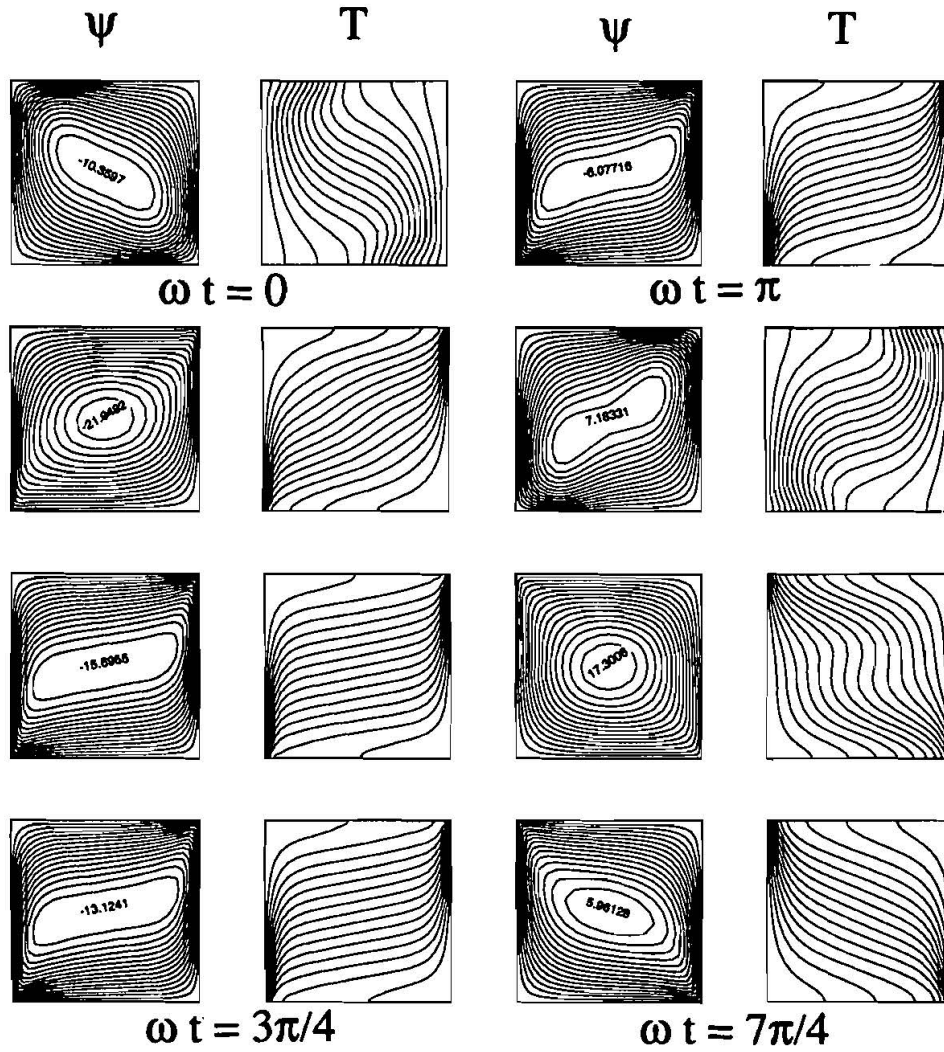


Figure 9. Time sequence of ψ and T at $Ra = 200$, $Ra_v = 500$, and $f = 10$, over one cycle at intervals of $\omega t = \pi/4$.

Again, the main distinction from the case of viscous fluid is that in porous media there is no expressed resonance phenomenon; thus the complications characterized by the multiplicity of solutions around the resonance frequency [2, 15] are absent here. In addition, when the thermovibrational effect persists at high frequencies, as can be shown by application of the method of averaging in the case of fluid, there is no vibrational effect in porous media.

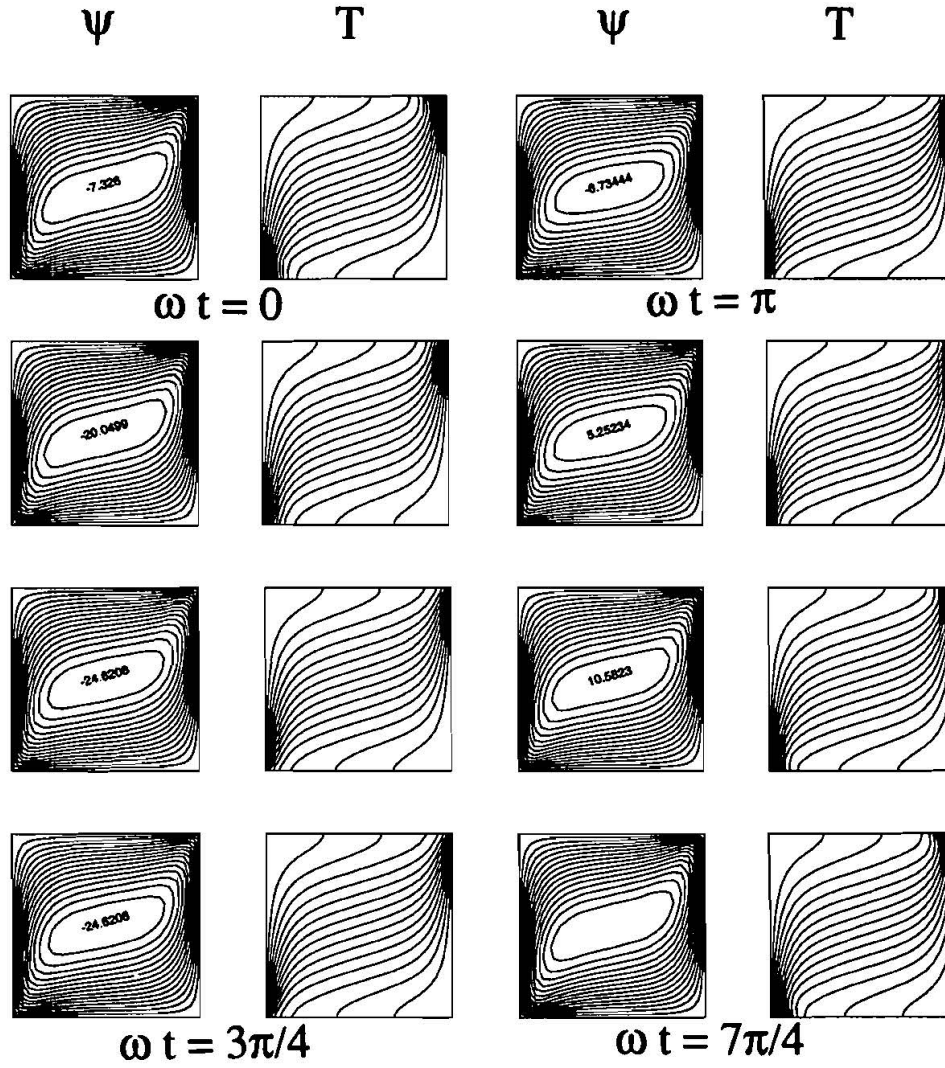


Figure 10. Time sequence of ψ and T at $Ra = 200$, $Ra_v = 500$, and $f = 400$, over one cycle at intervals of $\omega t = \pi/4$.

CONCLUSIONS

Convective oscillations are considered in porous media in a square, differentially heated cavity subject to vertical oscillations. The instantaneous and mean structures of the streaming flow are studied. A thermovibrational convection effect is shown even in the case of weightlessness. This effect disappears in the limiting case of high frequency.

The influence of convective oscillations on natural convection is also considered. When the vibrational Rayleigh number is high enough ($Ra_v/Ra \geq 2$), it is shown that significant modification of the streaming flow and heat transfer can be obtained in the range of low frequencies. The thermovibrational effect diminishes when the frequency is increased, whereas the basic natural convection flow is established in the limiting case of infinite frequencies (in the framework of the Darcy model).

REFERENCES

1. Yu. S. Yurkov, Vibrational Thermal Convection in Square Cavity in Weightlessness (Finite Frequencies), in *Convective Flows*, pp. 98–103, Perm, 1981.
2. G. Z. Gershuni, E. M. Zhukhovitsky, and Yu. S. Yurkov, Convective Oscillations in a Closed Cavity in Modulated Gravity Field, in *Convective Flows*, pp. 73–80, Perm, 1979.
3. G. Z. Gershuni and E. M. Zhukhovitsky, On Free Thermal Convection in Vibrational Field in Weightlessness, *Dokl. Akad. Nauk SSSR*, vol. 294, pp. 580–584, 1979.
4. G. Z. Gershuni and E. M. Zhukhovitsky, On Convective Instability of Fluid in Vibrational Field in Weightlessness, *Izv. Akad. Nauk SSSR Mekh. Zhidk. Gaza*, vol. 4, pp. 12–19, 1981.
5. H. R. Brand and V. Steinberg, Convective Instabilities in Binary Mixture in a Porous Medium, *Physica*, vol. 119A, pp. 327–338, 1983.
6. M. N. Ourzazi and P. A. Bois, Convective Instability of a Fluid Mixture in a Porous Medium with Time-Dependent Temperature Gradient, *Eur. J. Mech. B/Fluids*, vol. 13, no. 3, pp. 275–298, 1994.
7. A. F. Glukhov, D. V. Lyubimov, and G. F. Patin, Convective Motion in a Porous Medium near the Equilibrium Instability Threshold, *Sov. Phys. Dokl.*, vol. 23, pp. 22–25, 1978.
8. D. V. Lyubimov, *Dynamical Properties of Thermal Convection in Porous Medium: Instabilities in Multiphase Flows*, Plenum, New York, 1993.
9. J. P. Caltagirone and P. Fabrie, Natural Convection in a Porous Medium at High Rayleigh Numbers, Part I: Darcy's Model, *Eur. J. Mech. B Fluids*, vol. 8, pp. 207–227, 1989.
10. M. De la Torre Juárez and F. H. Busse, Stability of Two-Dimensional Convection in a Fluid Saturated Porous Medium, *J. Fluid Mech.*, vol. 292, pp. 305–323, 1995.
11. C. Canuto, M. Y. Hussaini, A. Quarteroni, and T. A. Zang, *Spectral Methods in Fluid Dynamics*, Springer Verlag, New York, 1987.
12. M. Azaiez, C. Bernardi, and M. Grundmann, Spectral Methods Applied to Porous Media, *East West J. Numer. Math.*, vol. 2, pp. 91–105, 1994.
13. M. Azaiez, F. Benbelgacem, and H. Khallouf, High Order Projection Schemes and Spectral Solution of the Incompressible Navier-Stokes Equations, *J. Math. Model. Numer. Anal.* (submitted).
14. A. Farooq and G. M. Homsy, Streaming Flows due to g-Jitter-Induced Natural Convection, *J. Fluid Mech.*, vol. 271, pp. 351–378, 1994.
15. H. Khallouf, Numerical Study of Thermovibrational Convection Using a Spectral Method, Ph.D. thesis, Université Paul Sabatier, Toulouse, France, 1995.